Results in Physics 26 (2021) 104419

Contents lists available at ScienceDirect

Results in Physics

journal homepage: www.elsevier.com/locate/rinp

Atomic population inversion in a two-level atom for shaped and chirped laser pulses: Exact solutions of Bloch equations with dephasing

S. Grira [a,*], N. Boutabba [b], H. Eleuch [c,d]

[a] Department of Applied Sciences and Mathematics, Abu Dhabi University, Abu Dhabi, United Arab Emirates
[b] Fatima College of Health Sciences, Institute of Applied Technology, Abu Dhabi, United Arab Emirates
[c] Department of Applied Physics and Astronomy, University of Sharjah, Sharjah, United Arab Emirates
[d] Institute for Quantum Science and Engineering, Texas A&M University, College Station, TX 77843, USA

ARTICLE INFO

Keywords:
Atomic population control
Two-level atom
Exact solutions
Chirped pulses

ABSTRACT

We perform a theoretical analysis of the Bloch equations of a two-level atom with dephasing. Exact analytical solutions with two different chirped and time-dependent detuned laser pulses are derived. The atomic population inversion as well as the coherence are explored for different initial populations. We show that the stationary population inversion can be controlled.

Introduction

In the field of light–matter interaction, the two-level system provides a simple way to strengthen the understanding of quantum optics. It is used as a basis framework to illustrate important light phenomena. In fact, when a powerful monochromatic laser stimulates such systems, they exhibit a fluorescence spectrum of three-peak structures known as the Mollow spectrum measured by heterodyne detection [1,2]. As for the case of the homodyne detection, the experimental squeezing of the fluorescent light was demonstrated [3]. Quantum information technologies [4] used the coherent control of a single two-level quantum system with electromagnetic fields. Therefore, an impressive progress has been made by controlling and measuring quantum bits in various physical systems including trapped ions [5], quantum dots [6–9], defects in solids [10], and superconducting quantum circuits [10]. Nonetheless, processing of the quantum computing by coherently controlling a qubit have a significant effect on the advancement of the quantum information field. This can be achieved by constructing a qubit (two-level system) that interacts with a time-dependent pulse [11, 12]. Furthermore, the two-level system provided a major insight into the development of superconducting circuits leading to a substantial outcome. It was used as a quantum sensor for absolute power calibration by measuring the spectrum of its dispersed radiation [13]. On the other hand, high-order non-linear optical phenomena were achieved [14–16] using the technique of femto-second laser chirping pulse amplification. Chirped pulses are very efficient for achieving and enhancing the atomic population inversion in atomic and molecular systems either by using coherent light–matter interactions like adiabatic rapid passage (ARP) [17] or by considering specific shaped pulses with a phase jump [18]. In a previous study, the case of a shaped exponential pulse was explored [19] , where the authors considered the simplest form of decoherence out of resonance, namely dephasing, and derived an exact analytical solution.

In our work, we derive exact analytical solutions for two new types of pulses: the modified form of the Tanh-hyperbolic pulse and the modified form of a quotient double exponential wave form. These two shaped pulses are assumed to excite the two-level atom for chirped frequencies. Such pulses have been used in numerical analysis as an analytical form of the pulse shapes of the high-altitude electromagnetic power (HEMP) and gamma-ray source [20,21]. The possible experimental implementation of such pulses is explained in [22]. In this paper, we show that for specific shaped pulses, we can achieve a high population transfer rate, which is critical in the realization of quantum memory. It is worth to mention that, chirping pulses is widely used in the CPA laser technique (chirped population amplification) to realize ultra-short lasers with extremely high-energy. Such pulses are very efficient in the implementation of the atomic population transfers in atoms and molecules [23]. Finally, our pulses are typically useful for specific realistic lasers, for instance the Tan-hyperbolic corresponds to a sudden switching on–off RF-pulse generator [24], while the modified Tan-hyperbolic pulse describes an input light that starts from an initial amplitude and drops suddenly with a fast fall time. From another side, the modified QEXP wave form is used in the HEMP and G-ray sources. Even though the exact solutions derived here in the two-level atom are

* Corresponding author.
E-mail address: grira.sofiane@adu.ac.ae (S. Grira).

https://doi.org/10.1016/j.rinp.2021.104419
Received 3 January 2021; Received in revised form 28 May 2021; Accepted 1 June 2021
Available online 5 June 2021

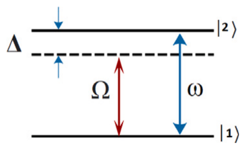

Fig. 1. The energy diagram of a two-level atom.

Table 1
The considered optical fields, the detunings, and the used change of variable x(t).

Case 1	Case 2
$\Omega = (\tanh(t) - 1)^2$	$\Omega = \frac{e^{-3\Gamma t}}{(1+e^{-2\Gamma t})^{\frac{3}{2}}}$
$\Delta = \mathrm{sech}^2(t)$	$\Delta = \Gamma \frac{e^{-2\Gamma t}}{(1+e^{-2\Gamma t})^{\frac{3}{2}}}$
$x = \tanh(t)$	$x = \frac{1}{\sqrt{e^{-2\Gamma t}+1}}$

fundamental, they might pave the way for implementations in many fields of quantum technology, including the realization of quantum memories and the development of light sources with exceptional optical properties on demand.

Here, we study a two-level atom, where we apply a strong light chirped pulse in the presence of a variable detuning. In section "Model", we derive exact analytical solutions for the atomic populations as well as the coherence between the ground and the excited state. Two pulses were considered: a modified form of the tan-hyperbolic pulse and a modified quotient exponential wave form. In section "Exact solutions of the atomic population inversion for chirped pulses" we analyse our results followed by concluding remarks.

Model

We consider a two-level atom described by a two-dimensional state space spanned by the two energy eigenstates $|1\rangle$ and $|2\rangle$ and atomic frequency ω_a. The atom interacts with a laser field with a frequency ω_f. The atom is subject to the dephasing. In many physical systems dephasing can occur, such as collective dephasing resulting from the inhomogeneous broadening of the atomic ensemble [25], collision dephasing in atomic gas [26] and atomic coherence dephasing generated by the laser pump field [27].

The considered two-level system interacting with an electromagnetic field is illustrated in Fig. 1.

The total system Hamiltonian in the interaction picture using the rotating-wave approximation can be written as

$$H = \Delta(t)\sigma_z \frac{\hbar}{2} + \Omega(t)\sigma_z \frac{\hbar}{2} \tag{1}$$

where σ_x, and σ_z represent the Pauli matrices. The part involving $\Omega(t)$ presents the time-dependent driving field. Note that the amplitude of the pulse is the Rabi frequency with the dimension of a frequency and proportional to the laser–atom interaction such as: $\Omega(t) = -d\frac{E(t)}{\hbar}$, where d is the dipole moment. $\Delta = \omega_2 - \omega_1$ designs the detuning which is time depending. The temporal evolution of the system is governed by the master equations of the Hermitian density matrix as:

$$\frac{d\rho(t)}{dt} = -i\,[H,\rho] + \frac{\Gamma}{2}(\sigma_z\rho\sigma_z - \rho) \tag{2}$$

with Γ is the dephasing rate inversely proportional to the decoherence time. Here, we investigate the atomic population inversion as well as the coherence in the two-level atom excited by a chirped and shaped laser fields. Our objective is to find the atomic population inversion $\rho_{inv} = \rho_{22} - \rho_{11}$ at $t = \infty$ by deriving exact analytical solutions to the density matrix elements under the rotating wave approximation.

The dynamics of the atomic populations and the coherences in terms of the Bloch equations are giving by:

$$\begin{bmatrix} \frac{du(t)}{dt} \\ \frac{dv(t)}{dt} \\ \frac{d\rho_{inv}(t)}{dt} \end{bmatrix} = \begin{bmatrix} -\Gamma & -\Delta(t) & 0 \\ \Delta(t) & -\Gamma & -\Omega(t) \\ 0 & \Omega(t) & 0 \end{bmatrix} \begin{bmatrix} u(t) \\ v(t) \\ \rho_{inv}(t) \end{bmatrix} \tag{3}$$

Here $\rho_{inv} = \rho_{22} - \rho_{11}$ denotes the atomic population inversion between the upper state $|2\rangle$ and the ground state $|1\rangle$ whereas $u(t)$ and $v(t)$ represent respectively the real and imaginary part of the temporal atom-field coherence $2\rho_{12}(t)$. (It is worth noting that u and v are also respectively related to the absorption and dispersion spectra if they are analysed in terms of the detunings).

Exact solutions of the atomic population inversion for chirped pulses

In this work we focus on two different cases of chirped pulses. The first one is a Tan-hyperbolic modified waveform while the other one is known as Pulsed modified form of exponential functions [22]. Physical parameters of the pulse such as the pulse rise time, full width at half maximum and full time are usually expressed as mathematical parameters related to the dimensionless parameter Γ in this analysis. Such, exponential waveforms are widely used to describe high power electromagnetic fields known as (HEMP) and ultra wide band pulses (UWB) [20]. Some modified exponential forms denoted as double exponential (DEXP), quotient exponential (QEXP) and power exponential (PEXP) have been widely used with physical parameters relevant to experimental situations [22]. Next, we derive exact analytical solutions for the atomic population inversion as well as the coherence. It is worth noting that, in a realistic case, one can only observe a temporal coherence if the pulsed duration of the field is shorter than the time constant of any decay mechanisms. In other terms, spontaneous radiative transitions disrupt coherence, hence in order to arrange an observable coherence, one must ensure that the interaction time between the field and the atom is shorter than the radiative decay constant. Here, we limit our study to the analytical analysis of exact solutions for the two cases detailed in Table 1.

In order to solve the system of differential equations describing the Bloch equations for the two chirped cases mentioned above, we introduce three new variables: v_1, u_1 and ρ_{inv1} related to the previous $u(t)$, $v(t)$ and $\rho_{inv}(t)$ as:

$$v_1(t) = v(t)e^{\Gamma t} \tag{4}$$

$$u_1(t) = u(t)e^{\Gamma t} \tag{5}$$

$$\rho_{inv1}(t) = \rho_{inv}(t)e^{\Gamma t} \tag{6}$$

By considering new change of variables $x = \int \Delta(t)dt$, and defining $g(x) = \frac{\Omega(x)}{\Delta(x)}$ and $h(x) = \frac{\Gamma}{\Delta(x)}$, Eq. (3) becomes:

$$\frac{du_1}{dx} = -v_1(x) \tag{7}$$

$$\frac{dv_1}{dx} = u_1(x) - g(x)\rho_{inv1}(x) \tag{8}$$

$$\frac{d\rho_{inv1}}{dx} = h(x)\rho_{inv1}(x) + g(x)v_1(x) \tag{9}$$

These coupled differential equations will be the basis of our further endeavour to determine the exact solutions for the two considered chirped pulses in Table 1.

Case 1: Modified tan-hyperbolic pulse

The input pulse (see Table 1) has the shape of a modified Tan-hyperbolic wave pulse. The Tan-hyperbolic pulse begins from $t = 0$ with an amplitude increasing towards the long-time asymptotic value 0. Such a behaviour of the input pulse is observed, e.g., after a sudden switching on–off RF-pulse generator [28]. In contrast, the modified Tan-hyperbolic form considered here, starts from an initial amplitude and drops suddenly with a fast fall time. (See Fig. 2.)

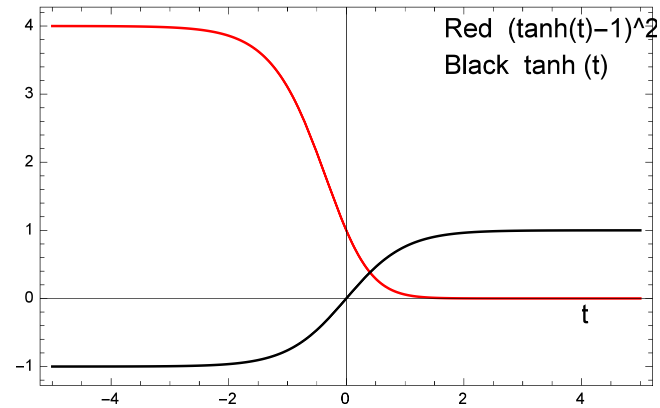

Fig. 2. The pulse shape: Tanh and modified Tan-hyperbolic wave forms.

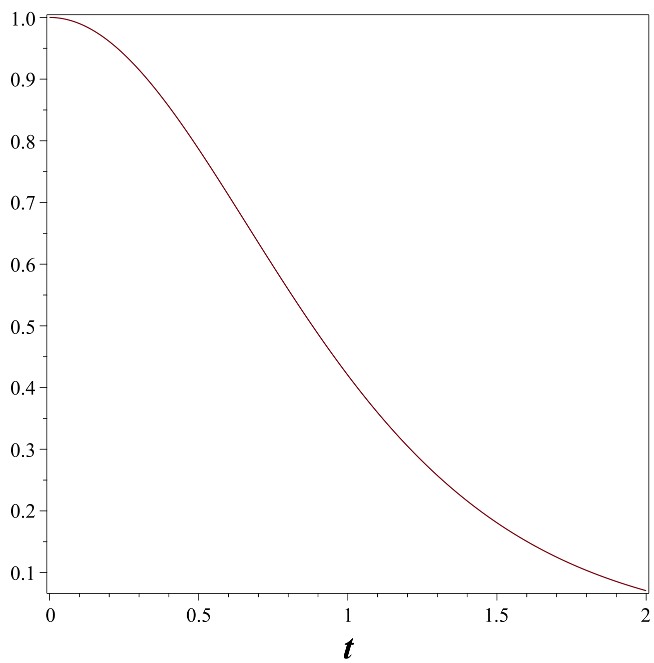

Fig. 3. Frequency detuning $\Delta(t) = \mathrm{sech}^2(t)$.

The frequency of the pump pulse is considered here as a time-dependent, the shape of the frequency detuning is illustrated in Fig. 3. It is worth mentioning that the time-dependent frequency detuning is used in the adiabatic population transfer for Raman systems [29,30].

We turn our attention now to the exact solution of Bloch Equations for this considered pulse.

By repeated differentiation and substitution of the last three Eqs. (7)–(9) we get a linear third-order ordinary differential equation

$$\frac{d^3u_1}{dx^3} + \left(\frac{2}{1+x}\right)\frac{du_1}{dx} = 0 \tag{10}$$

Solving the last equation leads to expressions of $u_1(t)$, $v_1(t)$ and ρ_{inv1} in terms of Bessel functions (type 1 and 2). Consequently the exact dynamical solutions of the coherence and population inversion can be determined. It is of great interest to derive the solutions in terms of initial conditions, since they may influence the atomic population inversion. We consider as initial conditions of the two-level system: $u(0) = 2\sqrt{A(1-A)}$, $v(0) = 0$, $\rho_{inv}(0) = 1-2A$ where A denotes the initial atomic population in the ground state $|1\rangle$. This gives:

$$\begin{aligned} u_1(t) = {} & c_1 + c_2(1+\tanh(t))J_2(2\sqrt{2+2\tanh(t)}) \\ & + c_3(1+\tanh(t))Y_2(2\sqrt{2+2\tanh(t)}) \end{aligned} \tag{11}$$

$$v_1(t) = \left(c_2 J_1(2\sqrt{2+2\tanh(t)}) + c_3 Y_1(2\sqrt{2+2\tanh(t)})\right)\sqrt{2+2\tanh(t)} \tag{12}$$

where

$$c_1 = -A + \sqrt{A(1-A)} + \frac{1}{2},$$

$$c_2 = \frac{Y_1\left(2\sqrt{2}\right)\left(2\sqrt{A(1-A)} + 2A - 1\right)}{-2J_0\left(2\sqrt{2}\right)Y_1\left(2\sqrt{2}\right) + 2J_1\left(2\sqrt{2}\right)Y_0\left(2\sqrt{2}\right)}$$

and

$$c_3 = \frac{J_1\left(2\sqrt{2}\right)\left(2\sqrt{A(1-A)} + 2A - 1\right)}{2J_0\left(2\sqrt{2}\right)Y_1\left(2\sqrt{2}\right) - 2J_1\left(2\sqrt{2}\right)Y_0\left(2\sqrt{2}\right)}$$

Then the time evolution of the real and imaginary parts of the coherence have the following expressions:

$$\begin{aligned} u(t) = {} & \sqrt{\frac{1-\tanh(t)}{1+\tanh(t)}}\left(c_1 + c_2(1+\tanh(t))J_2(2\sqrt{2+2\tanh(t)}) \right. \\ & \left. + c_3(1+\tanh(t))Y_2(2\sqrt{2+2\tan(t)}) \right) \end{aligned} \tag{13}$$

$$\begin{aligned} v(t) = {} & -\sqrt{\frac{1-\tanh(t)}{1+\tanh(t)}}\left(\left(c_2 J_1(2\sqrt{2+2\tanh(t)}) \right.\right. \\ & \left.\left. + c_3 Y_1(2\sqrt{2+2\tanh(t)}) \right)\sqrt{2+2\tanh(t)}\right) \end{aligned} \tag{14}$$

The dynamics of the atomic population inversion is governed by:

$$\begin{aligned} & \rho_{inv}(t) \\ & = \Big(2(KY_1(2\sqrt{2})(1+\tanh(t))J_1(2\sqrt{2+2\tanh(t)})) \\ & - KJ_1(2\sqrt{(2)})(1+\tanh(t))Y_1(2\sqrt{2+2\tanh(t)}) + \\ & \sqrt{2+2\tanh(t)}(-KY_1(2\sqrt{2})(\tanh(t)-1)J_0(2\sqrt{2+2\tanh(t)}) + \\ & KJ_1(2\sqrt{2})(\tanh(t)-1)Y_0(2\sqrt{2+2\tanh(t)}) - \\ & (-Y_1(2\sqrt{2})J_0(2\sqrt{2}) + Y_0(2\sqrt{2})J_1(2\sqrt{2}))(A - \sqrt{A(1-A)} - \frac{1}{2}))\Big) \times \\ & \frac{1}{\sqrt{2+2\tanh(t)}\left(-2Y_1(2\sqrt{2})J_0(2\sqrt{2}) + 2Y_0(2\sqrt{2})J_1(2\sqrt{2})\right)} \end{aligned} \tag{15}$$

where $K = A + \sqrt{A(1-A)} - \frac{1}{2}$. The stationary solution reads:

$$\begin{aligned} \rho_{inv}(\infty) = {} & \Big(((2Y_1(4) - 2Y_0(2\sqrt{2}))J_1(2\sqrt{2}) \\ & - 2Y_1(2\sqrt{2})(J_1(4) - J_0(2\sqrt{2})))\sqrt{A(1-A)} - \\ & 2((-Y_1(4) - Y_0(2\sqrt{2}))J_1(2\sqrt{2}) \\ & + Y_1(2\sqrt{2})(J_1(4) + J_0(2\sqrt{2})))(A - \frac{1}{2}) \Big) \\ & \frac{1}{\left(2Y_1(2\sqrt{2})J_0(2\sqrt{2}) - 2Y_0(2\sqrt{2})J_1(2\sqrt{2})\right)} \end{aligned} \tag{16}$$

The figures of $u(t)$ and $v(t)$ are displayed as 3D-plots representing the variation of the atomic coherence as function of the initial state and time. We observe that the coherence (more precisely both its real and imaginary parts which are linked respectively to the absorption and dispersion u and v) is almost independent of the initial state while the population inversion is sensitive to initial conditions (see Figs. 4 and 5). As the time evolves, the dispersion and absorption decrease.

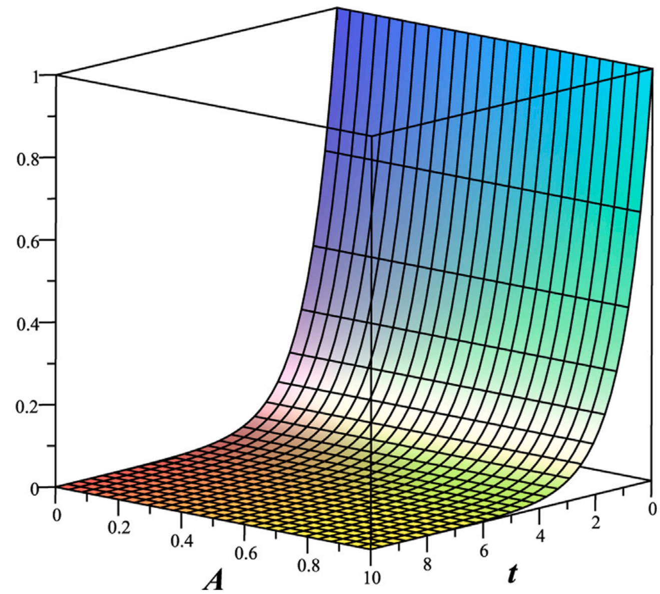

Fig. 4. 3D-plot of the absorption as a function of normalized time and initial population for pulse $\Omega = (\tanh(t) - 1)^2$ and detuning $\Delta = \mathrm{sech}^2(t)$.

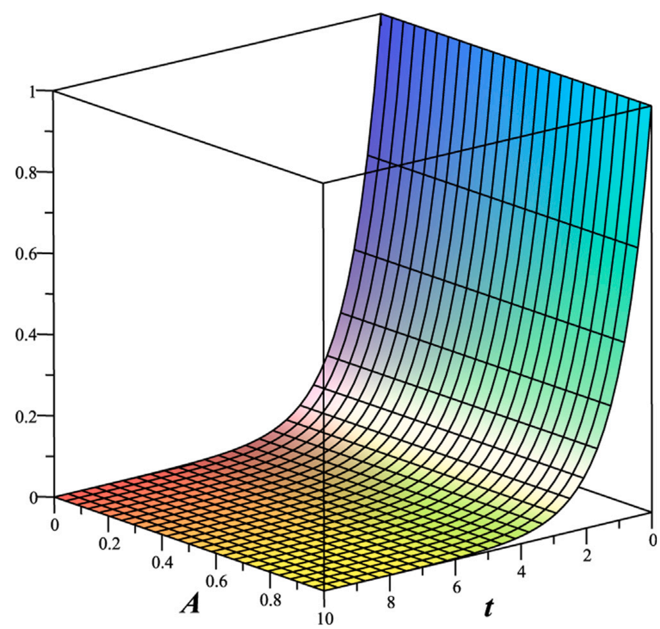

Fig. 5. 3D-plot of the dispersion as a function of normalized time and initial population for pulse and detuning same as Fig. 4.

The population inversion left is illustrated in Fig. 6. The stationary population inversion, $\rho_{inv}(\infty)$, is almost linear on the parameter A (representing the initial population at the ground state). The population inversion left is controlled by this initial condition and can be enhanced by stimulating the population in the excited state of the two-level system. We notice in this simulation that the dephasing rate is taken as a normalization factor ($\frac{1}{\Gamma} = 1$). By using this type of pulse shape and considering the initial population totally in the excited state, we find that 89.4% of the population is excited at infinity. Another significant case of possible importance in quantum metrology is that the system is initially in a coherent superposition of the two states ($A = \frac{1}{2}$). For this case we get a population inversion. The population distribution in the ground and the excited states are respectively 57.5% and 42.5%.

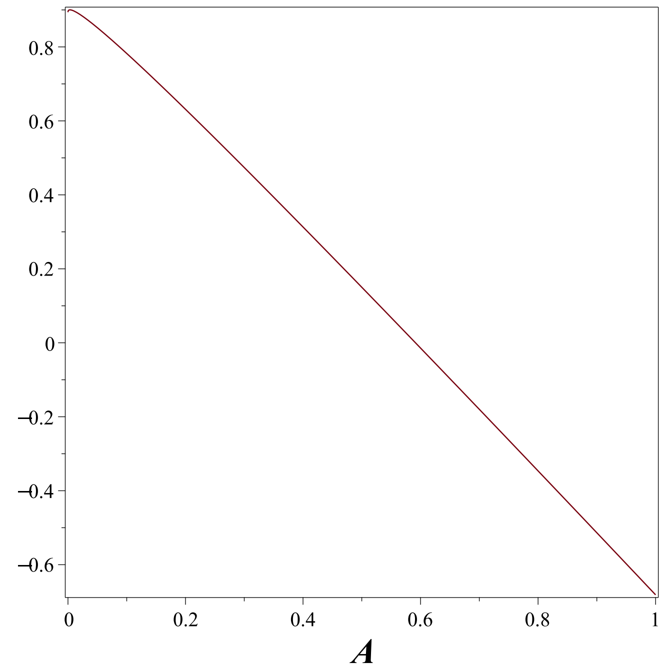

Fig. 6. Atomic population inversion Left $\rho_{inv}(\infty)$ for pulse and detuning same as Fig. 4.

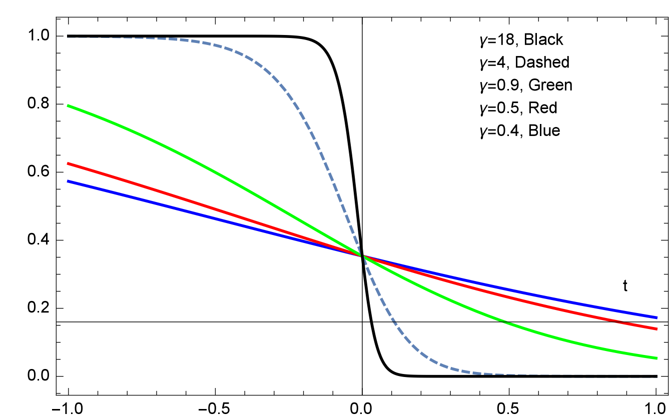

Fig. 7. Shapes of modified QEXP pulses.

Even though for A=1 the initial population is in the ground state, the left population distribution in the excited state represents 16%.

Case 2: modified quotient exponential pulse

For the second case where the two-level system is derived by a modified quotient exponential pulse (QEXP) in the form $\Omega = \frac{e^{-3\Gamma t}}{(1+e^{-2\Gamma t})^{\frac{3}{2}}}$ (Fig. 7 represents the time dependence of the pulse for different values of Γ) and with a time-variable detuning $\Delta = \Gamma \frac{e^{-2\Gamma t}}{(1+e^{-2\Gamma t})^{\frac{3}{2}}}$, the Bloch equations can be reduced after multiple differentiations and algebraic manipulations of the dynamical Eqs. (7)–(9) to the following differential equations describing the evolution of the modified real part of the coherence:

$$\frac{d^3u_1}{dx^3} + \frac{1}{x^2}\frac{du_1}{dx} = 0 \tag{17}$$

The solution of this equation with initial conditions $u(0) = 2\sqrt{A(1-A)}$, $v(0) = 0, \rho_{inv}(0) = 1 - 2A$ allows us to determine the time evolution of the population inversion as well as the dynamical expressions of the

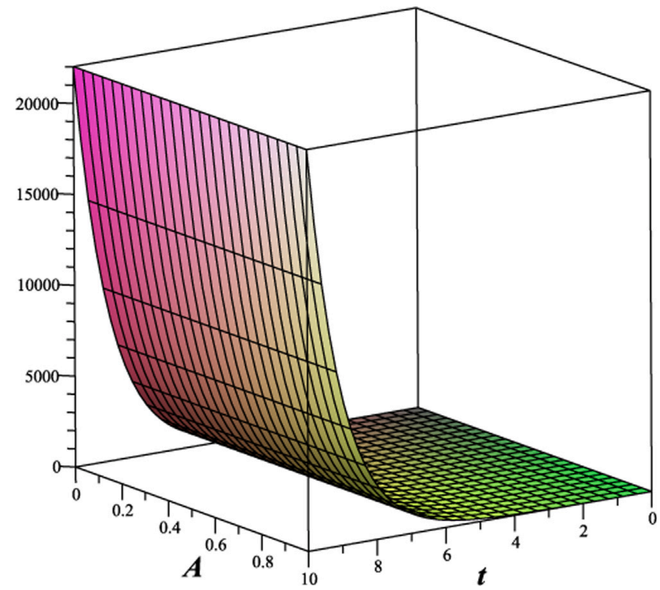

Fig. 8. 3D-plot of the real part of the coherence as a function of normalized time and initial population for pulse $\Omega = \frac{e^{-3\Gamma t}}{(1+e^{-2\Gamma t})^{\frac{3}{2}}}$, detuning $\Delta = \Gamma \frac{e^{-2\Gamma t}}{(1+e^{-2\Gamma t})^{\frac{3}{2}}}$ and $\Gamma = 1$.

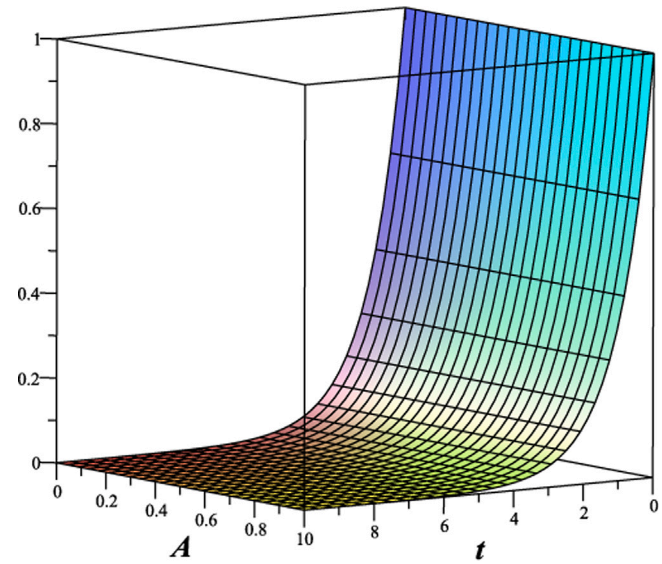

Fig. 9. 3D-plot of the imaginary part of the coherence as a function of normalized time and initial population for pulse, detuning and Γ same as Fig. 8.

coherence:

$$\rho_{inv}(x) = c_1 + c_2 x^{\frac{3}{2}} \sin\left(\frac{\sqrt{3}}{2}\ln x\right) + c_3 x^{\frac{3}{2}} \cos\left(\frac{\sqrt{3}}{2}\ln x\right) + \\ + \frac{c_2\sqrt{3}\cos\left(\frac{\sqrt{3}}{2}\ln x\right)}{\sqrt{x}} - \frac{c_3\sqrt{3}\sin\left(\frac{\sqrt{3}}{2}\ln x\right)}{\sqrt{x}} \tag{18}$$

$$u(x) = \frac{\sqrt{1-x^2}}{x}\left(c_1 + c_2 x^{\frac{3}{2}} \sin\left(\frac{\sqrt{3}}{2}\ln x\right) + c_3 x^{\frac{3}{2}} \cos\left(\frac{\sqrt{3}}{2}\ln x\right)\right) \tag{19}$$

$$v(x) = \frac{\sqrt{1-x^2}}{x}\left(-\frac{3}{2}c_2\sqrt{x}\sin\left(\frac{\sqrt{3}}{2}\ln x\right) - \frac{\sqrt{3}}{2}c_2\cos\left(\frac{\sqrt{3}}{2}\ln x\right) - \\ - \frac{3}{2}c_3\sqrt{x}\cos\left(\frac{\sqrt{3}}{2}\ln x\right) + \frac{\sqrt{3}}{2}c_3\sqrt{x}\sin\left(\frac{\sqrt{3}}{2}\ln x\right)\right) \tag{20}$$

where $x = \frac{1}{\sqrt{e^{-2\Gamma t}+1}}$, c_1, c_2 and c_3 are constants given by the expressions in Box I.

Figs. 8 and 9 are illustrated as 3D-plot of the real and imaginary parts of the atomic coherence in terms of the initial state and normalized time. As the time evolves, the real part of the coherence $u(t)$ increases while the imaginary part linked to the dispersion $v(t)$ decreases. u and v are pseudo-independent of the initial population distribution. Now, we are interested to analyse the behaviour of the population inversion as a function of the initial population. From Eq. (18) we deduce the expression of the atomic population inversion at infinity:

$$\rho_{inv}(\infty) = \frac{1}{3}\left(\sqrt{A(1-A)} + A - \frac{1}{2}\right)2^{\frac{3}{4}}\left(-2\cos\left(\frac{\sqrt{3}}{4}\ln 2\right) \\ - 2\sqrt{3}\sin\left(\frac{\sqrt{3}}{4}\ln 2\right)\right) + \\ \frac{1}{6} - \frac{A}{3} + \frac{5}{3}\sqrt{A(1-A)} \tag{21}$$

Fig. 10 represents the atomic population inversion left as function of the initial state. This plot shows us that $\rho_{inv}(\infty)$ is pseudo-linear on the population of the ground state.

This initial condition governs the remaining population inversion and can be improved by stimulating the population in the excited state of the two-level system. In this simulation, we note that the dephasing rate is taken as a normalization factor ($\frac{1}{\Gamma} = 1$).

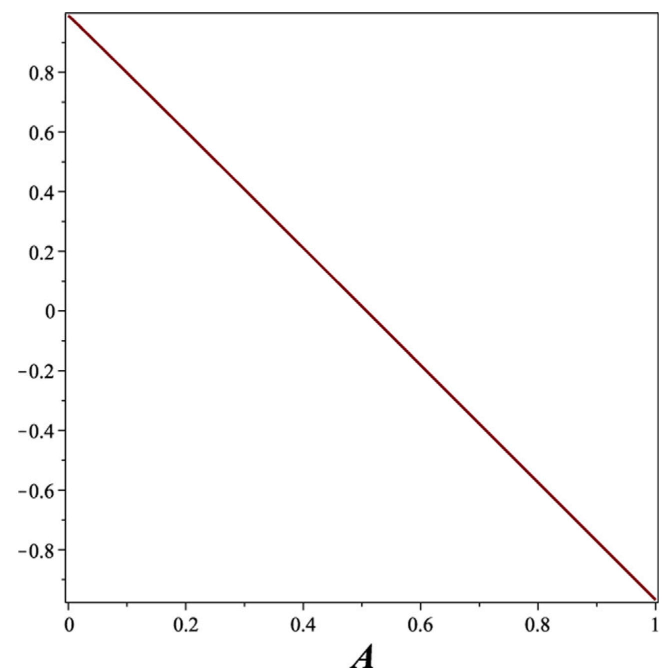

Fig. 10. Stationary atomic population inversion $\rho_{inv}(\infty)$ for Pulse, Detuning and Γ same as Fig. 8.

We found that 98.93% of the population is excited at infinity by using this form of pulse shape and considering the initial population entirely in the excited state. When the system is initially in a coherent superposition of the two states (A = $\frac{1}{2}$), the population inversion is almost vanishing. The population distribution in the ground and the excited states are respectively 50.75% and 49.25%. For A=1, we observe that the initial population is in the ground state and the left population distribution in the excited state represents 1.61%. Compared with the first case where the pulse has a modified Tan-hyperbolic form, we deduce that the current pulse generates more population inversion for an initial population totally distributed in the excited state. However, for

$$c_1 = -\frac{A}{3} + \frac{5\sqrt{A(1-A)}}{3} + \frac{1}{6},$$

$$c_2 = -\frac{\left(\sqrt{3}\sin\left(\frac{\sqrt{3}\ln(2)}{4}\right) + 3\cos\left(1/4\sqrt{3}\ln(2)\right)\right)2^{\frac{3}{4}}\sqrt{3}}{9} \times \left(\sqrt{A(1-A)} + A - \frac{1}{2}\right)$$

and

$$c_3 = \frac{2^{\frac{3}{4}}\left(2\sqrt{A(1-A)} + 2A - 1\right)\sqrt{3}\left(\sqrt{3}\cos\left(\frac{\sqrt{3}\ln(2)}{4}\right) - 3\sin\left(1/4\sqrt{3}\ln(2)\right)\right)}{18}$$

Box I.

other initial states the modified Tan-hyperbolic pulse is more adapted for producing stationary population in the excited state.

Conclusion

In this paper, we have investigated the effect of the light pulse shape on the control of the stationary atomic population inversion. By exploring the Bloch equations for two different chirped pulses with time-dependent frequency detuning, we have shown that we can control the atomic population dynamics by manipulating the light pulse and the initial population in the ground state. We have derived exact solutions for Modified Tan-hyperbolic and Modified Quotient Exponential pulses, considering the dephasing. We have shown that by using these pulses the population inversion can be conserved for a long time. Furthermore, for an initial population in the ground state, the stationary population distribution has a non-negligible part in the excited state, in particular for the modified quotient exponential pulse. We conclude that this pulse induces more population inversion for an initial population entirely in the excited state than the modified Tan-hyperbolic pulse, while Tan-hyperbolic pulse induces the reverse situation for other initial conditions. Thus, for other initial states, the modified Tan-hyperbolic pulse is more suitable for generating stationary populations in the excited state.

Declaration of competing interest

The authors declare that they have no known competing financial interests or personal relationships that could have appeared to influence the work reported in this paper.

References

[1] Höffges J, Baldauf H, Eichler T, Helmfrid S, Walther H. Heterodyne measurement of the fluorescent radiation of a single trapped ion. Opt Commun 1997;133(1–6):170–4.
[2] Wiseman H. Su (2) distribution functions and measurement of the fluorescence of a two-level atom. Quantum Semiclass Opt 1995;7(4):569–84.
[3] Lu Z, Bali S, Thomas J. Observation of squeezing in the phase-dependent fluorescence spectra of two-level atoms. Phys Rev Lett 1998;81(17):3635.
[4] Bennett CH, DiVincenzo DP. Quantum information and computation. Nature 2000;404(6775):247–55.
[5] Leibfried D, Blatt R, Monroe C, Wineland D. Quantum dynamics of single trapped ions. Rev Modern Phys 2003;75(1):281.
[6] Abdel-Aty AH, Kadry H, Mohamed ABA, Eleuch H. Correlation dynamics of nitrogen vacancy centers located in crystal cavities. Sci Rep 2020;10(1):1–11.
[7] Bonadeo NH, Erland J, Gammon D, Park D, Katzer D, Steel D. Coherent optical control of the quantum state of a single quantum dot. Science 1998;282(5393):1473–6.
[8] Press D, Ladd TD, Zhang B, Yamamoto Y. Complete quantum control of a single quantum dot spin using ultrafast optical pulses. Nature 2008;456(7219):218–21.
[9] Lodahl P, Mahmoodian S, Stobbe S. Interfacing single photons and single quantum dots with photonic nanostructures. Rev Modern Phys 2015;87(2):347.
[10] Weber J, Koehl W, Varley J, Janotti A, Buckley B, Van de Walle C, et al. Quantum computing with defects. Proc Natl Acad Sci 2010;107(19):8513–8.
[11] Eleuch H, Guérin S, Jauslin HR. Effects of an environment on a cavity-quantum-electrodynamics system controlled by bichromatic adiabatic passage. Phys Rev A 2012;85(1):013830.
[12] Tian M, Barber ZW, Fischer JA, Babbitt WR. Geometric manipulation of the quantum states of two-level atoms. Phys Rev A 2004;69(5):050301.
[13] Hönigl-Decrinis T, Shaikhaidarov R, de Graaf S, Antonov V, Astafiev O. Two-level system as a quantum sensor for absolute calibration of power. Phys Rev A 2020;13(2):024066.
[14] Kobtsev S, Kukarin S, Smirnov S, Turitsyn S, Latkin A. Generation of double-scale femto/pico-second optical lumps in mode-locked fiber lasers. Opt Express 2009;17(23):20707–13.
[15] Teubner U, Gibbon P. High-order harmonics from laser-irradiated plasma surfaces. Rev Modern Phys 2009;81(2):445.
[16] Wahlström C-G. High-order harmonic generation using high-power lasers. Phys Scr 1994;49(2):201.
[17] Attie H. Control of CO2 vibrational dynamics via shaped-pulse coherent anti-stokes Raman spectroscopy (Ph.D. thesis), Stellenbosch: Stellenbosch University; 2017.
[18] Boutabba N, Eleuch H. Quantum control of an optically dense atomic medium: Pulse shaping in a v-type three-level system. Results Phys 2020;19:103421.
[19] Zlatanov KN, Vasilev GS, Ivanov PA, Vitanov NV. Exact solution of the Bloch equations for the nonresonant exponential model in the presence of dephasing. Phys Rev A 2015;92(4):043404.
[20] Xie Y. Modified description of early time high-altitude electromagnetic pulse waveform (e1). Sens Simul Notes 2013;562.
[21] Baum CE. From the electromagnetic pulse to high-power electromagnetics. Proc IEEE 1992;80(6):789–817.
[22] Wu G. Shape properties of pulses described by double exponential function and its modified forms. IEEE Trans Electromagn Compat 2014;56(4):923–31.
[23] Fainberg BD, Gorbunov VA. Adiabatic rapid passage in molecules in solution excited by an intense ultrashort chirped pulse. In: Femtochemistry and femtobiology. 2004.
[24] Longmire CL, Hamilton RM, Hahn JM. A nominal set of high-altitude EMP environments. Tech. rep., Santa Barbara, CA (USA): Mission Research Corp.; 1987.
[25] Heinze G, Hubrich C, Halfmann T. Stopped light and image storage by electromagnetically induced transparency up to the regime of one minute. Phys Rev Lett 2013;111:033601.
[26] Sun Yong, Yang Yaping, Chen Hong, Zhu Shiyao. Dephasing-induced control of interference nature in three-level electromagnetically induced tansparency systems. Sci Rep 2015;5(1):16370.
[27] Chen JF, Zhang Weiping. Coherence time limit of the biphotons generated in a dense cold atom cloud. Sci Rep 2015;5(1):9126.
[28] Simeonov LS, Vitanov NV. Exactly solvable two-state quantum model for a pulse of hyperbolic-tangent shape. Phys Rev A 2014;89(4):043411.
[29] Dridi G, Guérin S, Hakobyan V, Jauslin HR, Eleuch H. Ultrafast stimulated Raman parallel adiabatic passage by shaped pulses. Phys Rev A 2009;80(4):043408.
[30] Guérin S, Thomas S, Jauslin HR. Optimization of population transfer by adiabatic passage. Phys Rev A 2002;65(2):023409.